

## THE STABILITY OF Fe-Mg CHLORITES IN HYDROTHERMAL SOLUTIONS: II. THERMODYNAMIC PROPERTIES

STEPHEN U. AJA

Department of Geology, Brooklyn College of the City University of New York, Brooklyn, NY 11210-2889, USA

**Abstract**—The hydrothermal stabilities of a low-Fe clinochlore and a high-Mg chamosite, in the presence of kaolinite, were investigated recently at  $T \leq 200^\circ\text{C}$  and  $P_\text{v} = P_{\text{H}_2\text{O}}$  (Aja and Small, 1999; Aja and Dyar, 2002). Standard state thermodynamic properties ( $S^0_{298}$ ,  $\Delta_f H^0_{1,298}$  and  $\Delta_f G^0_{1,298}$ ) have been obtained for the two chlorites whose structural formulae are  $(\text{Al}_{2.33}\text{Fe}^{2+}_{1.00}\text{Fe}^{3+}_{0.14}\text{Ca}_{0.02}\text{Mn}_{0.01}\text{Ni}_{0.02}\text{Cr}_{0.01}\text{Mg}_{8.40}\square_{0.07})(\text{Si}_{5.66}\text{Al}_{2.34})\text{O}_{20}(\text{OH})_{16}$  and  $(\text{Fe}^{3+}_{0.60}\text{Fe}^{2+}_{5.43}\text{Mg}_{2.30}\text{Al}_{2.98}\text{Mn}_{0.05}\text{Ca}_{0.03}\text{Zn}_{0.01}\square_{0.60})(\text{Si}_{5.63}\text{Al}_{2.37})\text{O}_{20}(\text{OH})_{16}$ . For the low-Fe clinochlore, the respective thermochemical properties are  $430 \text{ J mol}^{-1} \text{ K}^{-1}$ ,  $-8770.64 \pm 35.24 \text{ kJ mol}^{-1}$ , and  $-8120.54 \pm 32.63 \text{ kJ mol}^{-1}$ .  $\Delta_f H^0_{1,298}$ ,  $\Delta_f G^0_{1,298}$  and  $S^0_{298}$ , similarly obtained for the Windsor chamosite are  $-7851.29 \pm 23.14 \text{ kJ mol}^{-1}$ ,  $-7271.01 \pm 21.43 \text{ kJ mol}^{-1}$  and  $668 \pm 5 \text{ J mol}^{-1} \text{ K}^{-1}$ , respectively. Ideal site-mixing models of chlorite composition, along the chamosite-clinochlore binary, fail to model satisfactorily these chlorite-fluid equilibria only at lower temperatures ( $T < 175^\circ\text{C}$ ). The magnitudes of the excess thermodynamic properties calculated for these chlorites, within the ternary clinochlore-daphnite-sudoite system, suggest significant deviations from ideality.

**Key Words**—Chamosite, Clinochlore, Solid-solution, Sudoite, Thermodynamic Properties.

### INTRODUCTION

A number of activity-composition models have been employed to model compositional variations in chlorites (Stoessell, 1984; Walshe, 1986; Holland *et al.*, 1998; Vidal *et al.*, 2001). Stoessell formulated a random, regular-solution site-mixing model based on a set of six end-member component phases (amesite  $[(\text{Mg}_4\text{Al}_2)(\text{Si}_2\text{Al}_2)\text{O}_{10}(\text{OH})_8]$ , chamosite  $[(\text{Fe}^{2+}_4\text{Al}_2)(\text{Si}_2\text{Al}_2)\text{O}_{10}(\text{OH})_8]$ ,  $\text{Fe}^{3+}$ -chamosite  $[(\text{Fe}^{2+}_4\text{Fe}^{3+}_2)(\text{Si}_2\text{Al}_2)\text{O}_{10}(\text{OH})_8]$ , talc-3 brucite  $[(\text{Mg}_6)(\text{Si}_4)\text{O}_{10}(\text{OH})_8]$ , minnesotaite-3  $\text{Fe}(\text{OH})_2[(\text{Fe}^{2+}_6)(\text{Si}_4)\text{O}_{10}(\text{OH})_8]$ , pyrophyllite-2 gibbsite  $[(\text{Al}_4)(\text{Si}_4)\text{O}_{10}(\text{OH})_8]$ ; these end-members were ideal 14 Å chlorites for which thermochemical properties were not known. Activity-compositional models for chlorites have also been framed in terms of ideal site-mixing models (Helgeson and Aagaard, 1985); this presumes that compositional variation in the solid-solution is not accompanied by exchange of atoms between energetically distinct sites, and that the distribution of atoms is random on energetically equivalent sites. The ideal site-mixing model has been used rather extensively (Walshe, 1986; Jahren and Aagaard, 1992; Saccoccia and Seyfried, 1994). Walshe (1986), for instance, implemented an ideal site-mixing model for chlorites from hydrothermal systems based on a set of six end-member components  $(\text{Mg}_6\text{Si}_4\text{O}_{10}(\text{OH})_8)$ ,  $(\text{Mg}_5\text{Al}_2\text{Si}_3\text{O}_{10}(\text{OH})_8)$ ,  $(\text{Fe}^{2+}_5\text{Al}_2\text{Si}_3\text{O}_{10}(\text{OH})_8)$ ,  $(\text{Fe}^{2+}_5\text{Fe}^{3+}_2\text{Si}_3\text{O}_{10}(\text{OH})_8)$ ,  $(\text{Al}_4\text{Si}_4\text{O}_{10}(\text{OH})_8)$ ,  $(\text{Fe}^{2+}_4\text{Fe}^{3+}_1\text{Al}_2\text{Si}_3\text{O}_{11}(\text{OH})_7)$ . By contrast, Holland *et al.* (1998) proposed a model which permits mixing of atoms on energetically distinct structural sites and a variable degree of cation

ordering amongst the end-members: Al-free chlorite  $(\text{Mg}_6\text{Si}_4\text{O}_{10}(\text{OH})_8)$ , clinochlore  $[\text{Mg}_6\text{Si}_4\text{O}_{10}(\text{OH})_8]$ , amesite  $[(\text{Mg}_4\text{Al}_2)(\text{Si}_2\text{Al}_2)\text{O}_{10}(\text{OH})_8]$  and daphnite  $[(\text{Fe}^{2+}_5\text{Al})(\text{Si}_3\text{Al})\text{O}_{10}(\text{OH})_8]$ . This model, proposed in an effort to harmonize predicted and experimental compositional dependence on temperature for the chlorite + forsterite + orthopyroxene assemblage under elevated  $P$ - $T$  conditions, presumed a rather simple chlorite chemistry  $[(\text{R}_{6-x}^{2+}\text{Al}_x)(\text{Si}_{4-x}\text{Al}_x)\text{O}_{10}(\text{OH})_8]$  and the absence of octahedral vacancies in the 2:1 layer. But as noted by Vidal *et al.* (2001), octahedral vacancies in chlorites formed at temperatures  $< 450^\circ\text{C}$  are not artifacts of mixed layering. Hence, they proposed a 3-site mixing model having symmetric Margules parameters and ideal inter-site interaction. Their model is applicable to a wider  $P$ - $T$  range and presumes that octahedral vacancies result from di-trioctahedral substitutions, that all Fe is divalent, and that compositional variation in natural chlorites may be projected to the compositional space bounded by clinochlore, daphnite, amesite and Mg-sudoite  $[(\text{Si}_3\text{Al})(\text{Al}_3\text{Mg}_2)\text{O}_{10}(\text{OH})_8]$ . However, the Margules parameters for interaction on all sites except for  $M1$  were fixed *a priori* and thus restrict the mixing of the phase components on the  $M1$  site. As is to be expected, some overlap exists in the choice of end-members for the various activity-composition models though there is much less latitude in the choice of appropriate Fe end-members, especially  $\text{Fe}^{3+}$  minerals. Moreover, the simplifying assumptions required to implement the more robust models (Holland and Powell, 1996; Holland *et al.*, 1998; Vidal *et al.*, 2001) attest to the persistent need for additional experimental determinations of thermochemical properties of natural chlorites.

\* E-mail address of corresponding author:  
emenike\_nduozo@msn.com

In a prior contribution, Aja and Dyar (2002) presented the results of the experimental investigations of the relative stability of natural Fe-Mg chlorites (a low-Fe clinochlore and a high-Mg chamosite) in hydrothermal solutions. These experimental studies demonstrated that: (1) chlorite-fluid equilibrium is attainable under low temperature and/or diagenetic conditions; (2) appropriate solubility models for chlorite-fluid equilibria may be developed using the law of mass action (solubility constant approach); and (3) slopes of chemical potential diagrams may constrain the identity of solubility-limiting phases. These compositionally complex natural chlorites behaved as single-phase, single-component micas of fixed compositions during solution equilibration experiments (see Appendix). But because chlorites are compositionally complex minerals whose behavior over the course of geological time, as opposed to the time-frame of an experimental investigation, may be best viewed as a solid-solution, it is instructive to examine the implications of these recent low-temperature solution equilibration data for chlorite solid-solution. In this contribution, therefore, standard state thermodynamic properties will be retrieved for the two natural chlorites and the implications of the solution equilibration data will also be evaluated in terms of the ideal site mixing model of chlorite solid solution.

## RESULTS

The overall structural formulae for the two chlorites used in the study are  $(\text{Al}_{2.33}\text{Fe}^{2+}_{1.00}\text{Fe}^{3+}_{0.14}\text{Ca}_{0.02}\text{Mn}_{0.01}\text{Ni}_{0.02}\text{Cr}_{0.01}\text{Mg}_{8.40}\square_{0.07})(\text{Si}_{5.66}\text{Al}_{2.34})\text{O}_{20}(\text{OH})_{16}$  and  $(\text{Fe}^{3+}_{0.60}\text{Fe}^{2+}_{5.43}\text{Mg}_{2.30}\text{Al}_{2.98}\text{Mn}_{0.05}\text{Ca}_{0.03}\text{Zn}_{0.01}\square_{0.60})(\text{Si}_{5.63}\text{Al}_{2.37})\text{O}_{20}(\text{OH})_{16}$ . These compositions conform to the general formulae,  $(\square_z R_u^{2+} R_y^{3+})(\text{Si}_{4-x}\text{Al}_x)\text{O}_{10}(\text{OH})_8$

where the number of octahedral vacancies ( $z$ ) is given by  $(y - x)/2$  and  $u + y + z = 6$  (Wiewióra and Weiss, 1990). Thus, whereas the low-Fe clinochlore is clearly a tri-trioctahedral chlorite ( $z < 0.5$ ; Wiewióra and Weiss, 1990), the identity of the Windsor chamosite (di-tri-, or tri-dioctahedral chlorite) is not resolved owing to lack of detailed knowledge of the distribution of the octahedral vacancy. A putative structural chemistry for the chlorites (Table 1) presumes, in the first instance, that the  $M4$  and  $T2$  sites were fully occupied by Al and Si and that all octahedral vacancies are assignable to the  $M1$  site (cf. Vidal *et al.*, 2001). The atomic proportion of  $\text{Fe}^{2+}$  in the  $M1$  site was then estimated using Mössbauer spectroscopic data (Aja and Dyar, 2002) and the balance of the  $M1$  site occupancy was assigned to Mg. The  $M1$  site assignments invariably pre-dispose the occupancies of the  $M2+M3$  site inasmuch as  $M4$  occupancy is somewhat certain. Though vacancies may well exist in the interlayer hydroxide sheet (Wiewióra and Weiss, 1990) and Mössbauer data cannot be relied upon to ascertain Fe site assignments (Aja and Dyar, 2002), the assignments nonetheless reflect the prevailing understanding of chlorite chemistry (cf. Welch *et al.*, 1995; Holland *et al.*, 1998).

Equilibrium constants retrieved from the solubility data, as a function of temperature, have been summarized in the Appendix (Table A1); details of experimental techniques and results have been reported previously (Aja and Small, 1999; Aja and Dyar, 2002). The apparent free energy of formation of the chlorites under isothermal, isobaric conditions ( $\Delta_a G_{chte,T}^0$ ) were calculated from the relation,

$$\Delta_a G_{chte,T}^0 = -\Delta G_{reaction}^0 + \sum_i \Delta_a G_{i,T}^0 \quad (1)$$

where  $\Delta G_{reaction,T}^0$  and  $\sum_i \Delta_a G_{i,T}^0$  are the free energy of reaction (equal to  $-2.303 RT \log K$ ) and the apparent

Table 1. Some properties of the two natural chlorites.

Putative structural chemistry of two natural chlorites							
	$T1$	$T2$	$M1$	$M4$	$(M2 + M3)$		
Low-Fe clinochlore	$\text{Si}_2$	$(\text{Si}_{0.83}\text{Al}_{1.17})$	$(\square_{0.03}\text{Mg}_{0.941}\text{Fe}_{0.029}^{2+})$	Al	$(\text{Mg}_{3.259}\text{Al}_{0.17}\text{Fe}_{0.471}^{2+}\text{Fe}_{0.07}^{3+}\text{Ca}_{0.01}\text{Ni}_{0.01}\text{Cr}_{0.01})$		
Windsor chamosite	$\text{Si}_2$	$(\text{Si}_{0.72}\text{Al}_{1.28})$	$(\square_{0.30}\text{Fe}_{0.342}^{2+}\text{Mg}_{0.385})$	Al	$(\text{Mg}_{0.792}\text{Al}_{0.49}\text{Fe}_{0.30}^{3+}\text{Fe}_{2.378}^{2+}\text{Mn}_{0.03}\text{Ca}_{0.01})$		
Mole fraction ( $X$ )	Low-Fe clinochlore			Windsor chamosite			
$X_{\text{clinochlore}}$	0.820			0.200			
$X_{\text{daphnite}}$	0.118			0.602			
$X_{\text{sudoite}}$	0.062			0.198			
Gibbs free energy of formation from the elements ( $\text{kJ mol}^{-1}$ )	$\Delta_f G_{T,P}^0 = (a - e)T - aT\ln T + d - \frac{bI^2}{2} - \frac{c}{2T}; \quad 25 \leq T \leq 200^\circ\text{C}$ and $P_v = P_{\text{H}_2\text{O}}$						
$a \times 10^2$	Low-Fe clinochlore						
$b \times 10^{-2}$	-0.5006						
$c$	5.6378						
$d$	-4869312						
$e \times 10^2$	18838						
	2.8980						
	Windsor chamosite						
	1.7053						
	-26.456						
	9053346						
	-77314						
	-9.4564						

Gibbs energy of reactants and/or species (Table A2) in the solubility models, respectively. The standard state Gibbs free energy of formation from the elements ( $\Delta_f G_{chte,T}^0$ ) of the reacted chlorites were then calculated using the Gibbs energy function (Robie and Hemingway, 1995) and the relation,

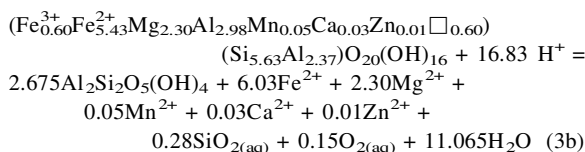
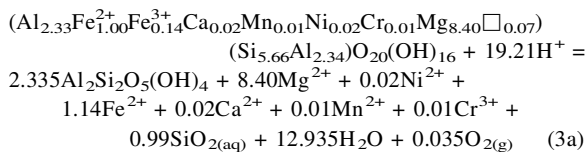
$$\Delta_f G_{chte,T}^0 \supseteq \Delta_a G_{chte,T}^0 - \left[ \sum_{j=1}^n \left( \frac{G_T^0 - H_{T_r}^0}{T} \right) \bullet T - \sum_{j=1}^n \left( \frac{G_{T_r}^0 - H_{T_r}^0}{T_r} \right) \bullet T_r \right] \quad (2)$$

Fit parameters for polynomials defining the functional dependence of  $\Delta_f G_{T,P}^0$  on temperatures (at saturated vapor pressures) are given in Table 1. The sequential retrieval of  $\Delta_f G_{chte,T}^0$  via  $\Delta_a G_{chte,T}^0$  (equations 1 and 2) assures consistency with the geochemical computer code (EQ3/6; Wolery, 1993) used in aqueous speciation analyses (Aja and Dyar, 2002); the latter relies on the revised HKF equations of state for aqueous ions and related thermochemical data (Shock and Helgeson, 1988; Johnson *et al.*, 1992).

## DISCUSSION

### Generalized solubility model

That a multiplicity of solubility models is needed to rationalize the behavior of the two chlorites in aqueous solutions is evident from Table A1 (Appendix) and reflects the deliberate omission of oxygen and pH buffers in the experimental charges as well as the effects of temperature on the properties of aqueous electrolytes, lability of reactions, aqueous geochemistry of iron and trace element content of the chlorites. Certainly, the multiplicity of the models yields important insights into the complexity of the reaction mechanisms but it also precludes a strict comparison of the thermal properties of the reactions. The latter requires derivation of a generalized solubility model for each chlorite (equation 3) from the experimental data; *i.e.*



Equation 3 presumes that Al is conserved in the solid phases and that all redox species exist in the reduced state; though these are standard assumptions, they lead to stoichiometric, and hence mass balance, constraints rather different from those inferred directly from the experi-

mental data (Table A1; Appendix). Inasmuch as thermochemical properties (*e.g.*  $\Delta_f G_{chte,T}^0$ ; Table 1) of the chlorites have been derived from the solubility data, equation 3 thus provides a simplified but realistic basis for evaluating chlorite-kaolinite equilibria under diagenetic conditions. As is evident, the temperature dependence of the equilibrium constants (Figure 1) shows the inherent differences in the thermal characteristics of the reactions of the two chlorites with kaolinite. A visual inspection of the data (Figure 1) suggests a linear dependence of  $\log K$  on inverse temperature and this is indeed the case for the Windsor chamosite-kaolinite reaction;

$$\log K_{3b} = -49.72 + 20137/T \quad (r^2 = 0.98) \quad (4a)$$

Equation 4a is of the general form,

$$\log K = -\frac{\Delta H_r^0}{2.303RT} - \frac{\Delta S_r^0}{2.303R} \quad (4b)$$

For the Windsor chamosite-kaolinite reaction (equation 3b),  $\Delta H_r^0$  and  $\Delta S_r^0$  are respectively determined as  $-385.59\text{ kJ mol}^{-1}$  and  $-952.14\text{ J mol}^{-1}\text{ K}^{-1}$ , respectively. Hence, the ‘second law method’ yields for the Windsor chamosite,  $\Delta_f G_{298,1}^0$  and  $S_{298}^0$  (from  $\Delta_f G^0 + \sum_{i=1}^n S_i^0$ ) equal to  $-7851.29\text{ kJ mol}^{-1}$  and  $668\pm 5\text{ J mol}^{-1}\text{ K}^{-1}$ , respectively; the resulting standard state free energy of formation of the Windsor chamosite ( $-7267.87\text{ kJ mol}^{-1}$ ) is thus consistent with  $\Delta_f G_{1,298}^0$  ( $-7271.01\pm 21.43\text{ kJ mol}^{-1}$ ) determined independently of equation 2. By contrast to the Windsor chamosite, the presumption of an inverse, linear temperature-dependence of equilibrium constants for the low-Fe clino-chlore-kaolinite reaction (equation 3a, Figure 1) yielded an unrealistic  $S_{298}^0$ . Equation 5 provides a more satisfactory model; *i.e.*

$$\log K_{3a} = 520.87 - 14198/T - 168.20\log T \quad (r^2 = 0.99) \quad (5)$$

The standard enthalpy of formation for the clino-chlore was calculated with the  $\Delta H_r^0$  obtained using

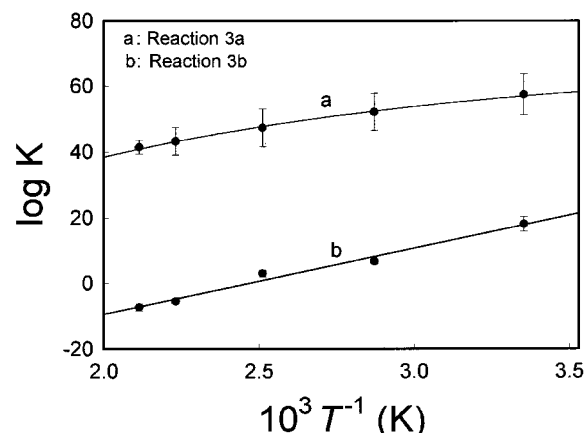


Figure 1. Equilibrium constants calculated for generalized chlorite-kaolinite solubility model (equation 3). (a) and (b) represent kaolinite-chlorite equilibrium with the low-Fe clino-chlore and Windsor chamosite, respectively.

equation 5. This, in conjunction with  $S_{298}^0$  obtained by polyhedral summation techniques ( $430 \text{ J mol}^{-1} \text{ K}$ ), were then used to adjust the standard free energy of formation ( $\Delta_f G_{1,298}^0$ ) obtained using equation 2. The standard state thermodynamic properties ( $\Delta_f H_{1,298}^0$ ,  $\Delta_f G_{1,298}^0$ ,  $S_{298}^0$ ) thus derived for the low-Fe clinochlore are  $-8770.64 \pm 32.63 \text{ kJ mol}^{-1}$ ,  $-8120.54 \pm 21.43 \text{ kJ mol}^{-1}$  and  $430 \text{ J mol}^{-1} \text{ K}^{-1}$ .

The data for the Windsor chamosite (Figure 3b) may certainly be modeled by presuming a non-linear temperature dependence of  $\log K$ ; this, however, presupposes a more complex model (*i.e.*  $\Delta C_{p,r} \neq 0$ ) than is required to explain the data. On balance, a curvilinear dependence of  $\log K_3$  on inverse temperature over the temperature range studied was expected for both chlorites given that these are rather complex heterogeneous reactions (*cf.* Nordstrom and Munoz, 1994; p. 222). Apparently, the fact that equation 3 is a net hydrolytic dissolution reaction, rather than a simple dissolution reaction, implies some compensating effects in the thermal properties of the chlorite-kaolinite reactions and hence the apparent flatness of the function,  $\frac{\partial \log K}{\partial (1/T)}$  over a temperature range of up to  $200^\circ\text{C}$ .

#### *Ideal site-mixing model of chlorite solid-solution*

Mineral compositional variations are amenable to various solid-solution treatments. Of the numerous solid-solution models, the ideal site-mixing model (Helgeson and Aagaard, 1985) has been widely utilized in studies of chlorites and illites found in diagenetic and hydrothermal assemblages and experimental systems (Bird and Norton, 1981; Walshe, 1986; Aagaard and Helgeson, 1983; Aagaard and Jahren, 1992; Saccoccia and Seyfried, 1994). In view of its demonstrated applicability to chlorite-fluid equilibria data at higher temperatures (Saccoccia and Seyfried, 1994), it is instructive to evaluate these recent chlorite solution equilibration data with the ideal site-mixing model. The activity ( $a_i$ ) of the  $i^{\text{th}}$  thermodynamic component of a solid-solution is given by,

$$a_i = k_i \prod_s \prod_j (X_{j,s})^{v_{s,j,i}} \quad (6)$$

where  $X_{j,s}$  is the mole fraction of the  $j^{\text{th}}$  atom on the  $s^{\text{th}}$  crystallographic site in the solid-solution,  $v_{s,j,i}$  is the stoichiometric number of the  $s^{\text{th}}$  sites occupied by the  $j^{\text{th}}$  atom in one mole of the  $i^{\text{th}}$  thermodynamic component and  $k_i$  is the proportionality constant,

$$k_i = \prod_s \prod_j (X_{j,s,i})^{v_{s,j,i}} \quad (7)$$

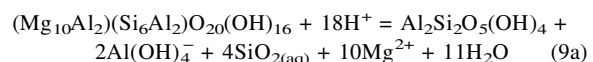
$X_{j,s,i}$  is the mole fraction of the  $j^{\text{th}}$  atom on the  $s^{\text{th}}$  crystallographic site in the  $i^{\text{th}}$  stoichiometric mineral. Based on equation 7, the proportionality constant for the low-Fe clinochlore and the Windsor chamosite are 148.60 and 234.34, respectively. Thus, for the thermodynamic components ( $\text{Mg}_5\text{Al}(\text{Si}_3\text{Al})\text{O}_{10}(\text{OH})_8$  and  $(\text{Fe}_5^{2+}\text{Al})(\text{Si}_3\text{Al})\text{O}_{10}(\text{OH})_8$ ,

$$a_i = 148.60(X_{\text{Mg},\text{O}})^5(X_{\text{Al},\text{O}})(X_{\text{Si},\text{T}})(X_{\text{Si},\text{T}})^3 \quad (8a)$$

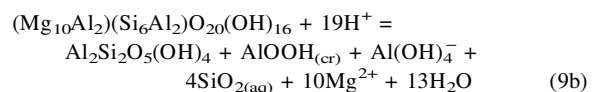
$$a_i = 234.34(X_{\text{Fe},\text{O}})^5(X_{\text{Al},\text{O}})(X_{\text{Al},\text{T}})(X_{\text{Si},\text{T}})^3 \quad (8b)$$

For the low-Fe clinochlore,  $\log a_{\text{clinochlore}}$  and  $\log a_{\text{daphnite}}$  are calculated (equation 8a) to be  $-0.30$  and  $-4.93$ , respectively. By contrast,  $\log a_{\text{clinochlore}}$  and  $\log a_{\text{daphnite}}$  for the Windsor chamosite calculated from equation 8b are  $-2.81$  and  $-0.94$ , respectively. Equation 8 implies that the different octahedral sites in the chlorite structure are homologous.

The binary clinochlore-daphnite system provides a framework for modeling chlorite solid-solution (Curtis, 1985; Hutcheon, 1990; Aagaard and Jahren, 1992) and hence the experimentally-measured chlorite-kaolinite reactions (Table A1, Appendix) resolve into the kaolinite-clinochlore and kaolinite-chamosite compatibilities. Hence, at  $T \leq 125^\circ\text{C}$  the appropriate reactions are



and at  $T \geq 175^\circ\text{C}$ ,



Though analogous reactions to equation 9 but containing daphnite may be derived easily, only the clinochlore components of the two natural chlorites were evaluated in this work owing to constraints imposed by the experimental data. Specifically, aqueous Fe was rarely present as  $\text{Fe}^{2+}$  in most of the runs (*cf.* Table A1) owing to the absence of redox potential buffers in the experimental charges and thus precludes a direct treatment of kaolinite-chamosite equilibria.

In Figure 2, values of  $\log(a_{\text{Mg}^{2+}}^{1/2})/(a_{\text{H}^+})$  calculated from equation 9, for the chlorite-kaolinite boundary (with the activity of the clinochlore phase components of the natural chlorites, equation 8), have been compared with values measured directly. For experiments conducted with low-Fe clinochlore (Figure 2a), the experimentally-measured kaolinite-chlorite boundary is more stable than the predicted one by nearly six orders of magnitude at  $25^\circ\text{C}$  whereas at  $200^\circ\text{C}$ , the values differ by  $\sim 0.4$  log units. A similar trend is observed for the chamosite data (Figure 2b) although at  $175^\circ$  (the highest temperature for which experimental data are available) the values differ by 1.5 log units. In other words, there is a virtual convergence of the experimental and theoretical values at  $200^\circ\text{C}$ . This suggests that at  $T \geq 200^\circ\text{C}$ , ideal site-mixing algorithms reasonably model these chlorite-fluid equilibria in the binary clinochlore-chamosite system. That the ideal site-mixing model satisfactorily predicts clinochlore-kaolinite equilibria under elevated temperature conditions is consistent with the findings of Saccoccia and Seyfried (1994) who similarly modeled their higher temperature ( $300$ – $500^\circ\text{C}$ ) chlorite solubility data with an ideal site-mixing model. They concluded

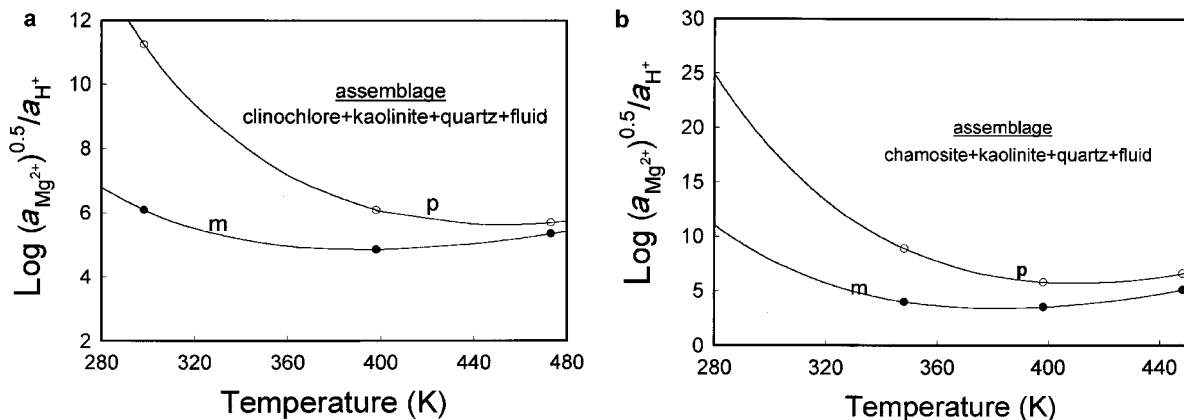


Figure 2. A comparison of predicted and measured  $\log(a_{\text{Mg}^{2+}}^{1/2}/a_{\text{H}^+})$  for chlorite-kaolinite-fluid assemblage projected to quartz saturation, between 25 and 200°C and at saturated vapor conditions. The predicted values presume an ideal site-mixing model for the chlorites (equations 8–9); smoothed values of the predicted (p) and measured (m) ion activity ratios, as a function of temperature, are indicated by the curves. The standard state thermodynamic properties of Robie and Hemingway (1995) for end-member clinochlore were used in the predictive model; the heat capacity data given in Table 2 were used for extrapolation to higher temperatures.

that an ideal site mixing model may rationalize their solubility data although a non-ideal model with a modest excess Gibbs energy ( $\Delta G^{\text{ex}} \approx 837 \text{ J mol}^{-1}$ ) was not precluded. At lower temperatures, however, the ideal site-mixing model fails to correctly reproduce the experimental data (Figure 2). The failure of the model under standard state conditions (25°C, 1 bar) is particularly significant inasmuch as other natural chlorites (e.g. the Vermont chlorite-kaolinite-quartz assemblage; Kittrick, 1982) equilibrate at a pH –  $\frac{1}{2}p\text{Mg}^{2+}$  value (6.5 at 25°C) comparable to the low-Fe clinochlore-kaolinite boundary (Figure 4a; Aja and Small, 1999). In other words, the limited data available indicate that other natural chlorites buffer values of  $\log(a_{\text{Mg}^{2+}}^{1/2}/a_{\text{H}^+})$  to values comparable to the ones measured in this study. The divergence of the predicted ion activity ratios from experimental data at lower temperatures (Figure 2) could stem from the following factors: metastability of

chlorite-kaolinite assemblages, erroneous standard state Gibbs free energy of formation for end-member chlorites, very large excess Gibbs energy for chlorite solid-solutions under low-temperature conditions or limitations of the ideal site-mixing model. A presumption of metastability of chlorite-kaolinite assemblages under lower temperature conditions is questionable given that the experimental charge should have buffered  $\log(a_{\text{Mg}^{2+}}^{1/2}/a_{\text{H}^+})$  to higher, rather than lower, values compared with the predicted values; moreover, the notion that the criteria used to assess equilibrium during the experiments could simultaneously indicate stable (at high temperatures) and metastable (at low temperatures) equilibrium is specious.

The apparent failure of the ideal site-mixing model under low-temperature conditions may also be partially attributed to uncertainties in standard state thermodynamic properties of end-member chlorites (clinochlore or daphnite). Though  $\Delta_f G_{298.1 \text{ bar}}^0$  reported by different investigators (cf. Table 2) fall within a standard deviation of 20 kJ mol<sup>-1</sup> (1σ), thermochemical values based on calorimetric data (e.g. Robie and Hemingway, 1995) are somewhat discrepant from those regressed from high-temperature, high-pressure phase equilibrium experiments (Berman, 1988; Holland and Powell, 1990, 1998). For the latter, linear regression approaches yield standard state properties different from those extracted using linear programming (Berman, 1988) techniques. In the former, the refined parameter is  $\Delta_f H_t^0$  whereas in the latter all parameters ( $\Delta_f H_t^0, s_0, V_0$ ) are minimized. Despite these differences, a presumption of an uncertainty of 20 kJ mol<sup>-1</sup> (in  $\Delta_f G_{298.1 \text{ bar}}^0$ ) shifts the calculated ion activity ratios by ~0.65 log units and even at the 2σ levels, a significant difference still exists between measured and predicted ion activity ratios. Indeed, to bring the predicted and measured  $\log(a_{\text{Mg}^{2+}}^{1/2}/a_{\text{H}^+})$  values into coincidence will require decreasing the

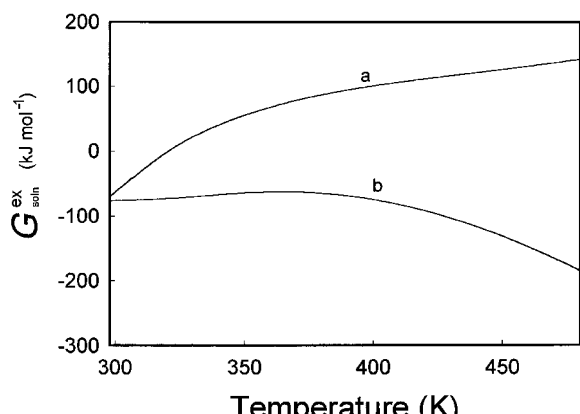


Figure 3. Variation of calculated excess Gibbs free energies (kJ mol<sup>-1</sup>) as a function of temperature. (a) and (b) show  $G_{\text{soln}}^{\text{ex}}$  calculated for the low-Fe clinochlore and Windsor chamosite, respectively.

Table 2. Thermodynamic properties of end-member chlorites\*.

Formula	$(\text{Mg}_5\text{Al})(\text{Si}_3\text{Al})\text{O}_{10}(\text{OH})_8$	$(\text{Fe}_5^{2+}\text{Al})(\text{Si}_3\text{Al})\text{O}_{10}(\text{OH})_8$	$(\square_1\text{Mg}_2\text{Al}_3)(\text{AlSi}_3)\text{O}_{10}(\text{OH})_8$
Name	clinochlore	$\text{Fe}^{2+}$ -chamosite/daphnite	sudoite
$\Delta_f H_{1,298}^0$	$-8919.9 \pm 20.0^{\text{a}}$	$-7101.97 \pm 4.17^{\text{b}}$	$-8634.36 \pm 1.86^{\text{c}}$
	$-8929.86 \pm 1.85^{\text{c}}$	$-7153.99 \pm 3.33^{\text{c}}$	
	$-8919.25 \pm 4.38^{\text{d}}$	$-7148.44 \pm 4.50^{\text{d}}$	
$\Delta_f G_{1,298}^0$	$-8255.8 \pm 20.0^{\text{a}}$	$-6495.13 \pm 4.17^{\text{b}}$	
	$-8263.35^{\text{c}}$	$-6535.56^{\text{c}}$	$-7976.77^{\text{c}}$
	$-8250.546^{\text{e}}$		
$S_{1,298}^0$	$421.00^{\text{a}}$	$559.00^{\text{b}}$	
	$410.50^{\text{c}}$	$545.00^{\text{c}}$	$399.00^{\text{c}}$
	$421.00^{\text{d}}$	$559.00^{\text{d}}$	
$V_{1,298}^0$	21.090	21.340	20.300
Heat capacity coefficients ( $C_p = a + bT - \frac{c}{T^2}$ )			
$a$	6.1279	6.0006	6.5638
$\Delta_f a$	0.3918	0.8228	1.0658
$b$	0.3151	0.3676	0.3843
$\Delta_f b$	0.1396	0.0755	0.2171
$c$	16873700	14441117	15840039
$\Delta_f c$	15652129	15253669	13627740

\* Sources of data: (a) Robie and Hemingway (1995); (b) Saccoccia and Seyfried (1993); (c) Holland and Powell (1998); (d) Holland and Powell (1990); (e) Berman (1988). Units:  $\Delta_f H_{1,298}^0$ ,  $\Delta_f G_{1,298}^0$ ,  $S_{1,298}^0$ ,  $V_{1,298}^0$ ,  $C_p$  are measured in  $\text{kJ mol}^{-1}$ ,  $\text{kJ mol}^{-1} \text{J mol}^{-1} \text{K}^{-1}$ ,  $\text{J bar}^{-1}$ ,  $\text{J mol}^{-1} \text{K}^{-1}$ , respectively. Heat capacity taken from Holland and Powell (1998).  $\Delta_f a$ ,  $\Delta_f b$ ,  $\Delta_f c$  are coefficients for the formation of the end-member chlorites from their constituent elements.

standard state Gibbs free energy of formation of clinochlore by up to 140  $\text{kJ mol}^{-1}$  ( $\Delta_f G_{298,1 \text{ bar}}^0 \approx -8396 \text{ kJ mol}^{-1}$ ).

In addition to uncertainties in standard state thermochemical properties, the inherent limitations of the ideal site-mixing model must be considered in any attempt to rationalize the divergence between predicted and measured ion activity ratios (Figure 2). A fundamental presumption of the ideal site-mixing model is mixing of atoms on energetically-equivalent sites, with consequent resolution of structural sites in chlorite solid-solution into tetrahedral and octahedral sites. This is clearly an approximation considering the multiplicity of cation sites in chlorites (Bailey, 1988; Welch *et al.*, 1995). These cation sites include two tetrahedral sites ( $T1$  and  $T2$ ), two octahedral sites in the TOT layer [ $M1$  (*trans*) and  $M2$  (*cis*)] and two octahedral sites in the interlayer ( $M3$  and  $M4$ ); these four distinct octahedral sites may accommodate  $\text{Fe}^{2+}$  or  $\text{Fe}^{3+}$  and atomic site occupancies for the  $M2$  and  $M3$  sites are not easily resolved for chlorites. Moreover, the distributions of Al and Si in tetrahedral sheets of chlorites are apparently highly ordered (Welch *et al.*, 1995). In spite of these structural chemistry imperatives, ideal mixing of atoms on homological sites describes compositional variation in chlorites at high temperatures; but at temperatures characteristic of diagenesis and low-temperature hydrothermal settings, the ideal site-mixing model fails to reproduce the experimental data. This pattern attests to the well established fact that with increased temperatures, there is a greater degree of freedom in the mixing of the components of a solid-solution; *i.e.* at low temperatures, the contribution of the enthalpy of

mixing ( $\Delta H_{\text{mix}}$ ) to the Gibbs energy of mixing greatly exceeds the entropy of mixing term ( $T\Delta S_{\text{mix}}$ ) suggesting either that a miscibility gap exists in the system, or that the chamosite (daphnite)-clinochlore binary join does not provide an adequate system for modeling diagenetic and/or hydrothermal chlorites. There is thus a need for more robust models, compared to the ideal site-mixing model, of chlorite solid-solutions. Though recent treatments of chlorite solid-solution contain the needed improvements (*e.g.* Holland *et al.*, 1998; Holland and Powell, 1996; Vidal *et al.*, 2001), an exact implementation of these latter models is constrained by available experimental data. For instance, the recognition that octahedral vacancies are real structural features of low-temperature chlorites (Vidal *et al.*, 2001; Wiewióra and Weiss, 1990) implies that consideration of sudoite (such as Mg-sudoite,  $(\square_1(\text{Mg}_2\text{Al}_3)(\text{AlSi}_3)\text{O}_{10}(\text{OH})_8)$ ) as an end-member mineral is particularly apposite in chlorite solid-solution models developed for low-temperature conditions. If possible contributions of  $\text{Fe}^{3+}$ -chamosite ( $(\text{Fe}^{3+}\text{Fe}^{2+})(\text{Si}_2\text{Al}_2)\text{O}_{10}(\text{OH})_8$ ) are justifiably omitted owing to the relatively small amount of  $\text{Fe}^{3+}$  present in the samples, the activity of the end-member phase components, clinochlore (cln), daphnite (daph) and Mg-sudoite (sud) may be given by (*cf.* Vidal *et al.*, 2001),

$$a_{\text{daph}} = 4(X_{\text{Si}}^{T2})(X_{\text{Al}}^{T2})(X_{\text{Fe}}^{M1})(X_{\text{Fe}}^{M2+M3})^4 \quad (10a)$$

$$a_{\text{cln}} = 4(X_{\text{Si}}^{T2})(X_{\text{Al}}^{T2})(X_{\text{Mg}}^{M1})(X_{\text{Mg}}^{M2+M3})^4 \quad (10b)$$

$$a_{\text{sud}} = 64(X_{\text{Si}}^{T2})(X_{\text{Al}}^{T2})(X^{M1})(X_{\text{Mg}}^{M2+M3})^2(X_{\text{Al}}^{M2+M3})^2 \quad (10c)$$

The non-ideal part of the excess function, given by equation 11, becomes

$$\begin{aligned} RT \ln \gamma_{\text{cln}} = & (X_{\text{Fe}}^2 + X_{\text{Fe}} X_{\text{Al}}) W_{\text{cln, daph}} + \\ & (X_{\text{Al}}^2 + X_{\text{Fe}} X_{\text{Al}}) W_{\text{cln, sud}} - X_{\text{Fe}} X_{\text{Al}} W_{\text{daph, sud}} \end{aligned} \quad (11a)$$

$$\begin{aligned} RT \ln \gamma_{\text{daph}} = & (X_{\text{Mg}}^2 + X_{\text{Mg, Al}}) W_{\text{cln, daph}} + \\ & (X_{\text{Al}}^2 + X_{\text{Mg}} X_{\text{Al}}) W_{\text{daph, sud}} - X_{\text{Mg}} X_{\text{Al}} W_{\text{cln, sud}} \end{aligned} \quad (11b)$$

$$\begin{aligned} RT \ln \gamma_{\text{sud}} = & (X_{\text{Fe}}^2 + X_{\text{Fe}} X_{\text{Al}}) W_{\text{daph, sud}} + \\ & (X_{\text{Mg}}^2 + X_{\text{Fe}} X_{\text{Mg}}) W_{\text{cln, sud}} - X_{\text{Fe}} X_{\text{Mg}} W_{\text{cln, daph}} \end{aligned} \quad (11c)$$

In equations 10 and 11,  $X$ ,  $\gamma$  and  $W$  represent the relevant mole fractions, activity coefficients and Margules parameters, respectively. A strict application of the above ternary model to the experimental data requires knowledge of the detailed structural chemistry of the chlorite samples particularly the amounts of cation ordering, the extent of intrasite and inter-site mixing within the various sites; these compositional parameters are unknown for the natural chlorites used in this study. Furthermore, the limited experimental data available under isothermal, isobaric conditions (from this investigation) constrain calculation of Margules' parameters even for a symmetric regular solution model. Though some Margules' parameters may be fixed independent of the system under investigation, this circumvents the need to demonstrate the efficacy of the model from first principles. Moreover, the data from this study cannot be augmented with independent solution equilibration data for other natural chlorites (at  $200^\circ\text{C} \geq T \leq 25^\circ\text{C}$ ;  $P_v = P_{\text{H}_2\text{O}}$ ) inasmuch as such complementary data are lacking. Clearly, the need for additional multilateral experimental investigations of chlorite-fluid equilibria under these low-temperature conditions cannot be overemphasized.

#### *Excess thermodynamic functions*

That chlorite solid-solutions exhibit significant deviation from ideality under low temperatures is indicated from the foregoing and thus an evaluation of the magnitudes of excess thermodynamic properties (such as Gibbs energy) serves important heuristic purposes. The excess Gibbs energy ( $G_{\text{soln}}^{\text{ex}}$ ) for chlorite solid-solution may be obtained from equation 12,

$$G_{\text{soln}}^{\text{ex}} = G_{\text{s.s.}}^0 - (\sum_i X_i G_i^0 - RT \sum_i X_i \ln X_i) \quad (12)$$

where,  $G_i^0$ ,  $G_{\text{s.s.}}^0$  and  $X_i$  represent the molar Gibbs free energy of the end-members, the molar free energy of formation of chlorite solid-solutions (calculated from experimental data) and mole fraction of the components in the solid-solutions, respectively. Mole fraction ( $X_i$ ) of the end-member phase components may be defined either as a thermodynamic mole fraction or molecular mole fraction. The former applies if mixing of atoms is random on energetically-equivalent sites whereas molecular mole fraction applies if local charge balance is maintained in the structure of the mineral. As previously noted, cation occupancies in the chlorite structure exhibit short-range ordering and thus validate adoption of molecular mole fraction.  $\Delta_f G_{T,P}^0$  for the end-member

minerals (clinochlore, daphnite, sudoite) used in this study were calculated from,

$$\begin{aligned} \Delta_f G_{T,P}^0 = & \Delta_f G_{\text{Tr,Pr}}^0 - \Delta_f S_{\text{Tr,Pr}}^0 (T - T_r) + \\ & \Delta_f a [T - T_r - T \ln \left( \frac{T}{T_r} \right)] + 0.5 \Delta_f b (2TT_r - T^2 - T_r^2) + \\ & 0.5 \Delta_f c (T^2 + T_r^2 - 2TT_r) T^{-1} T_r^{-2} + V_{1,298}^0 (P - 1) \end{aligned} \quad (13)$$

In equation 13,  $\Delta_f a$ ,  $\Delta_f b$ ,  $\Delta_f c$  (Table 2) are the Maier-Kelley heat capacity parameters for the formation of the end-member chlorites from their elements and the other quantities have their usual meanings. The excess Gibbs energy thus calculated (*i.e.* equation 12) for the low-Fe clinochlore and high-Mg chamosite are summarized in Figure 3. In either case, the excess Gibbs energy shows a varying degree of temperature dependence and given that the compositions of each chlorite are constant over the temperature range investigated, these excess functions are apparently dominated by enthalpy contributions. The magnitudes of the excess Gibbs energy imply significant deviation from ideality; the low-Fe clinochlore shows (for the most part) a positive departure from ideality whereas the high-Mg chamosite is characterized by a strongly negative deviation. Though these excess energies apply to molecular solid-solutions rather than strictly to pairwise interatomic interactions, their magnitudes nonetheless suggest rather large Margules parameters.

#### CONCLUSIONS

In recent experimental investigations (Aja and Small, 1999; Aja and Dyar, 2002), the hydrothermal stabilities of a low-Fe clinochlore and a high-Mg chamosite, in the presence of kaolinite, were investigated under diagenetic conditions ( $T \leq 200^\circ\text{C}$ ,  $P_v = P_{\text{H}_2\text{O}}$ ). Standard state thermodynamic properties ( $S_{298}^0$ ,  $\Delta_f H_{1,298}^0$  and  $\Delta_f G_{1,298}^0$ ), for these natural chlorites, have been obtained from these solution equilibration data. Equilibrium constants measured for the reactions of these two chlorites with kaolinite have inherently different temperature dependencies; whereas the chamosite-kaolinite reaction shows a linear dependence on inverse temperature, the clinochlore-kaolinite reaction is typified by a curvilinear dependence. In either case, nonetheless, the differential changes in  $\log K$  concomitant with differential changes in inverse temperature is a rather flat function and results from the compensating effects in the thermal properties of the reactions. At higher temperatures ( $T \geq 200^\circ\text{C}$ ), the experimental data are modeled satisfactorily with an ideal site-mixing model of chlorite solid-solution whereas the same model fails at lower temperatures. Apparently,  $\Delta H_{\text{mix}}$  greatly exceeds the  $T\Delta S_{\text{mix}}$  term as the temperature is decreased. Application of a more robust, internally consistent solid-solution model is, however, constrained by available data; additional studies designed to advance experimental calibration of chlorite solid-solution models must

necessarily include detailed structural chemistry of the natural chlorites being investigated, the use of sulfide fugacity buffers to control redox potential in addition to several components of the present chlorite-fluid equilibration experiments.

#### ACKNOWLEDGMENTS

This study was supported by a grant from the Petroleum Research Fund administered by the American Chemical Society (ACS-PRF# 29930-AC2) and by the University Committee on Research Awards (PSC-CUNY; RF# 6-66205, 6-667208) Program. Helpful comments by an anonymous journal reviewer are also acknowledged.

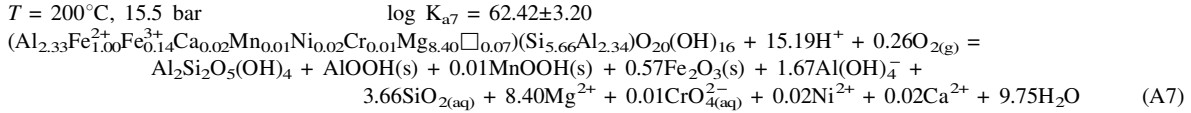
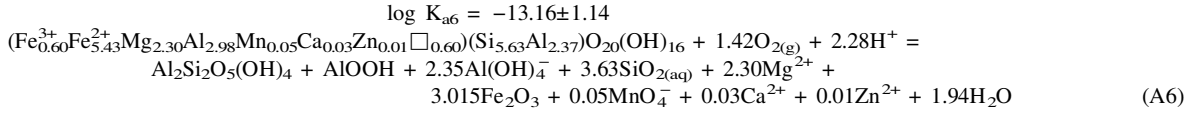
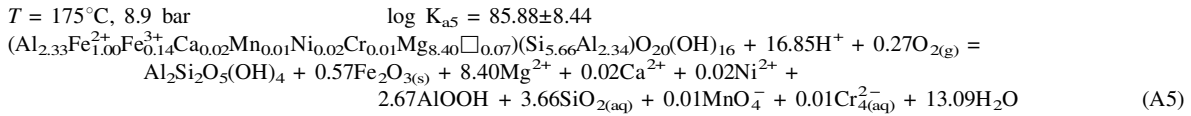
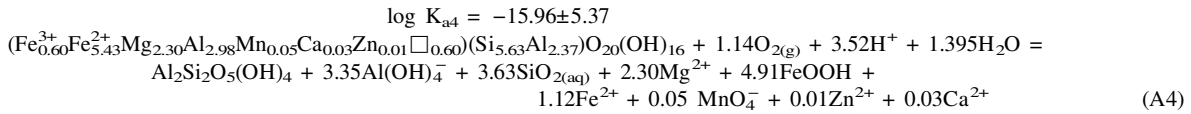
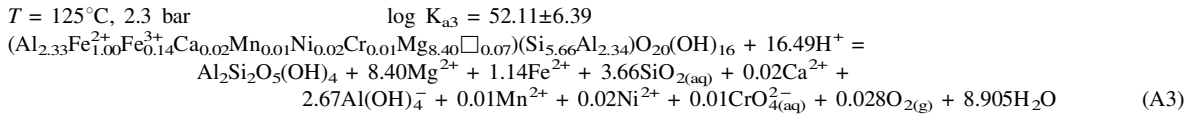
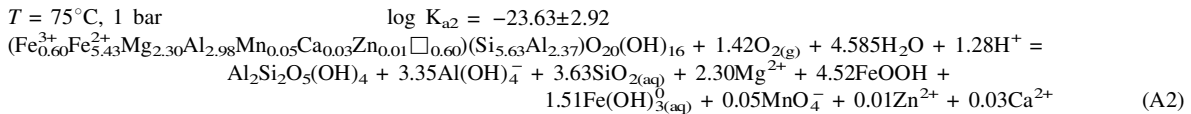
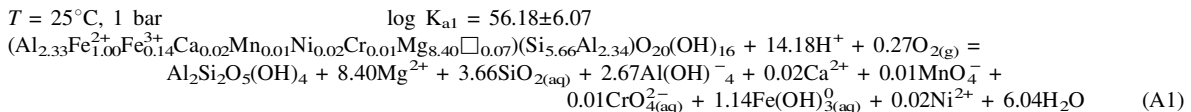
#### REFERENCES

- Aagaard, P. and Helgeson, H.C. (1983) Activity/composition relations among silicates and aqueous solutions: II. Chemical and thermodynamic consequences of ideal mixing of atoms on homologous sites in montmorillonites, illites, and mixed-layer clays. *Clays and Clay Minerals*, **31**, 207–217.
- Aagaard, P. and Jahren, J.S. (1992) Diagenetic illite-chlorite assemblages in arenites. II. Thermodynamic relations. *Clays and Clay Minerals*, **40**, 547–554.
- Aja, S.U. and Dyar, D.M. (2002) The stability of Fe-Mg chlorites in hydrothermal solutions: I. Results of experimental investigations. *Applied Geochemistry*, **17**, 1219–1239.
- Aja, S.U. and Small, J.S. (1999) The solubility of a low-Fe clinochlore between 25 and 175°C and  $P_v = P_{H_2O}$ . *European Journal of Mineralogy*, **11**, 829–842.
- Bailey, S.W. (1988) Chlorites: structure and crystal chemistry. Pp. 347–404 in: *Hydrous Phyllosilicates* (S.W. Bailey, editor). Reviews in Mineralogy, **19**. Mineralogical Society of America, Washington, D.C.
- Berman, R.G. (1988) Internally-consistent thermodynamic data set for minerals in the system Na<sub>2</sub>O-K<sub>2</sub>O-CaO-MgO-FeO-Fe<sub>2</sub>O<sub>3</sub>-Al<sub>2</sub>O<sub>3</sub>-SiO<sub>2</sub>-TiO<sub>2</sub>-H<sub>2</sub>O-CO<sub>2</sub>. *Journal of Petrology*, **29**, 445–522.
- Bird, D.K. and Norton, N.L. (1981) Theoretical prediction of phase relations among aqueous solutions and minerals: Salton Sea geothermal system. *Geochimica et Cosmochimica Acta*, **45**, 1479–1483.
- Curtis, C.D. (1985) Clay mineral precipitation and transformation during burial diagenesis. *Philosophical Transactions of the Royal Society of London*, **A 315**, 91–105.
- Helgeson, H.C. and Aagaard, P. (1985) Activity/composition relations among silicates and aqueous solutions: I. Thermodynamics of intrasite mixing and substitutional order/disorder in minerals. *American Journal of Science*, **285**, 769–844.
- Holland, T.J.B. and Powell, R. (1990) An enlarged and updated internally consistent thermodynamic dataset with uncertainties and correlations: the system K<sub>2</sub>O-Na<sub>2</sub>O-CaO-MgO-MnO-FeO-Fe<sub>2</sub>O<sub>3</sub>-Al<sub>2</sub>O<sub>3</sub>-TiO<sub>2</sub>-SiO<sub>2</sub>-C-H<sub>2</sub>-O<sub>2</sub>. *Journal of Metamorphic Geology*, **8**, 89–124.
- Holland, T.J.B. and Powell, R. (1996) Thermodynamics of order-disorder in minerals: II. Symmetric formalism applied to solid solutions. *American Mineralogist*, **81**, 1425–1437.
- Holland, T.J.B. and Powell, R. (1998) An internally-consistent thermodynamic data set for phases of petrological interest. *Journal of Metamorphic Geology*, **16**, 309–343.
- Holland, T., Baker, J. and Powell, R. (1998) Mixing properties and activity-composition relationships of chlorites in the system MgO-FeO-Al<sub>2</sub>O<sub>3</sub>-SiO<sub>2</sub>-H<sub>2</sub>O. *European Journal of Mineralogy*, **10**, 395–406.
- Hutcheon, I. (1990) Clay-carbonate reactions in the Venture area, Scotian Shelf, Nova Scotia, Canada. Pp. 199–212 in: *Geochemical Society Special Publication 2* (R.J. Spencer and I.-Ming Chou, editors). Geochemical Society, Washington, D.C.
- Jahren, J.S. and Aagaard (1992) Diagenetic illite-chlorite assemblages in arenites. II. Thermodynamic relations. *Clays and Clay Minerals*, **40**, 547–554.
- Johnson, J.W., Oelkers, E.H. and Helgeson, H.C. (1992) SUPCRT92: A software package for calculating the standard molar thermodynamic properties of minerals, gases, aqueous species and reactions from 1 to 5000 bars and 0 to 1000°C. *Computers and Geosciences*, **18**, 899–947.
- Kittrick, J.A. (1982) Solubility of two high-Mg and two high-Fe chlorites using multiple equilibria. *Clays and Clay Minerals*, **30**, 167–179.
- Nordstrom, D.K. and Munoz, J.L. (1994) *Geochemical Thermodynamics*. Blackwell Scientific Publications. Boston, Massachusetts, 493 pp.
- Robie, R.A. and Hemingway, B.S. (1995) Thermodynamic properties of minerals and related substances at 298.15 K and 1 bar ( $10^5$  Pascals) pressure and at higher temperatures. *United States Geological Survey Bulletin*, **2131**, 461 pp.
- Saccoccia, P.J. and Seyfried, Jr., W.E. (1993) A resolution of discrepant thermodynamic properties for chamosite retrieved from experimental and empirical techniques. *American Mineralogist*, **78**, 607–611.
- Saccoccia, P.J. and Seyfried, Jr., W.E. (1994) The solubility of chlorite solid solutions in 3.2 wt% NaCl fluids from 300–400°C, 500 bars. *Geochimica et Cosmochimica Acta*, **58**, 567–585.
- Shock, E.L. and Helgeson, H.C. (1988) Calculation of the thermodynamic and transport properties of aqueous species at high pressures and temperatures: correlation algorithms for ionic species and equation of state predictions to 5 kb and 1000°C. *Geochimica et Cosmochimica Acta*, **52**, 2009–2036.
- Stoessell, R.K. (1984) Regular solution site-mixing model for chlorites. *Clays and Clay Minerals*, **32**, 205–212.
- Vidal, O., Parra, T. and Trottet, F. (2001) A thermodynamic model for Fe-Mg aluminous chlorite using data from phase equilibrium experiments and natural pelitic assemblages in the 100–600°C, 1–25 kb range. *American Journal of Science*, **301**, 557–592.
- Walshe, J.L. (1986) A six-component chlorite solid solution model and the conditions of chlorite formation in hydrothermal and geothermal systems. *Economic Geology*, **81**, 681–703.
- Welch, M.D., Barras, J.B. and Klinowski, J. (1995) A multinuclear NMR study of clinochlore. *American Mineralogist*, **80**, 441–447.
- Wiewióra, A. and Weiss, Z. (1990) Crystallochemical classifications of phyllosilicates based on the unified system of projection of chemical composition: II. The chlorite group. *Clay Minerals*, **25**, 83–92.
- Wolery, T.J. (1993) *EQ3/6, A software package for geochemical modeling of aqueous systems (version 7.2)*. Lawrence Livermore National Laboratory UCRL-MA 110662.

(Received 19 September 2001; revised 1 March 2002; Ms. 586)

## APPENDIX

Table A1. Solubility models for chlorite-kaolinite equilibria\*.



\* Solution equilibration data of the two natural chlorites reported elsewhere (Aja and Small, 1999; Aja and Dyar, 2002). For presumptions of solubility models, see Aja and Dyar (2002). Equilibrium constants at a given temperature and pressure ( $K_T$ ) calculated using the relation,  $K_T = \frac{1}{n} \sum_{i=1}^n \prod a_i^{v_i}$  where  $a_i$ ,  $v_i$ ,  $n$  denote the activity of aqueous ions as calculated by EQ3/6, stoichiometric reaction coefficients and the number of data points that constrain the kaolinite-chlorite boundary, respectively.

Table A2. Apparent Gibbs free energy of formation ( $\Delta_a G_{T,P,i}^0$ ).

	$a \times 10^2$	$\Delta_a G_{T,P}^0 = (a - e)T - aT\ln T + d - \frac{bT^2}{2} - \frac{c}{2T}$	$d$	$e \times 10^2$
Boehmite	0.8416	-1.1863	-904104	-928846
Diaspore	0.3334	-3.8972	505722	-922091
Gibbsite	0.6697	15.0041	639520	-1163248
Goethite	0.6731	0.3032	-81290	-492818
Hematite	0.9531	8.3116	1350267	-755920
Kaolinite	2.6037	16.4886	5924468	-3842580
$\text{Al(OH)}_4^-$	14.3004	-256.38	49924177	-1752468
$\text{Ca}^{2+}$	4.9391	-110.42	16954830	-724736
$\text{Fe}^{2+}$	5.8875	-126.54	20723872	-311981
$\text{Fe(OH)}_{3,\text{(aq)}}^0$	5.3367	-57.87	11708932	-805784
$\text{H}_2\text{O}$	0.9317	-3.04	918076	-245807
$\text{CrO}_4^{2-}$	22.6534	-475.99	97623705	-1503941
$\text{Mn}_4^-$	9.1470	-177.81	35695632	-703510
$\text{Mg}^{2+}$	6.5010	-134.26	22893775	-706237
$\text{Ni}^{2+}$	-19.4496	357.59	-90414425	650148
$\text{SiO}_{2\text{(aq)}}^0$	0.5934	1.2149	1679678	-844092
$\text{Zn}^{2+}$	5.7510	-123.54	19735078	-362823

$\Delta_a G_T^0$  values (J mol<sup>-1</sup>) are based on SUPCTR92 (Johnson *et al.*, 1992) and apply to saturation vapor pressures and  $T < 250^\circ\text{C}$ .